Modeling Chlorite−Iodide Reaction Dynamics Using a Chlorine Dioxide−Iodide Reaction Mechanism

Maryam Jowza and Simeen Sattar*

Bard College, Annandale-on-Hudson, New York 12504-5000

Robert J. Olsen*

Division of Natural and Mathematical Sciences, The Richard Stockton College of New Jersey, Pomona, New Jersey 08240-0195

Received: September 16, 2004

The mechanism of Lengyel, Li, Kustin, and Epstein (*J. Am. Chem. Soc.* **1996**, *118*, 3708) for the oscillatory chlorine dioxide−iodide reaction accurately models the reaction in closed and open systems. We investigated whether this mechanism minus the single reaction involving chlorine dioxide models the chlorite−iodide reaction equally well. It agrees qualitatively with clock reaction results. As for open system dynamics, the mechanism predicts the existence of two steady states and bistability in very nearly the same regions where these features are found experimentally in the pH range 2−4. A discrepancy in the range of bistability emerges as pH decreases, and it cannot be remedied by taking into account chlorous acid decomposition. That we were unable to locate an oscillatory region is of greater significance. Because the chlorite−iodide reaction is sensitive to mixing effects, we incorporated a two-parameter model of imperfect mixing but still found no oscillations at physically reasonable parameter values. These discrepancies strongly suggest that to obtain predictive utility for the chlorite−iodide reaction, revision of the chlorine dioxide−iodide mechanism is required.

Introduction

Nearly twenty-five years after it was discovered,[1] the chlorite−iodide reaction remains one of the most fascinating oscillating reactions. It involves only two small ions, chlorite and iodide, in acidic aqueous solution. When these reagents are mixed together in a closed vessel, a classic clock reaction ensues. The solution turns yellow at an increasing rate as iodine forms and then suddenly becomes colorless; at the same instant, the iodide concentration plummets. When the reagents are flowed continuously into a stirred, constant-volume vessel (a CSTR), the system can exist in one of two distinct steady states and exhibit hysteresis between them (bistability), exist in an oscillatory state, or exhibit hysteresis between steady and oscillatory states. Of the two commonly observed steady states, one has a low iodide concentration resulting from high conversion and the other a high iodide concentration due to low conversion. A third steady state with intermediate iodide concentration has also been reported.[2,3] When reagents are mixed before entering the CSTR or the stirring rate is varied,[2,4−6] the bistable and oscillatory regions shift. These studies have planted the doubt that oscillations might be a consequence of imperfect mixing and therefore not inherent to the reaction kinetics.

Constructing a mechanism to account for the behavior of the chlorite−iodide reaction was, of course, an early goal. The first detailed mechanism, developed by Epstein and Kustin,[7] consists of thirteen reactions, two rapid equilibria, and nine reactive species. Although their mechanism generates clock behavior, bistability, and oscillations, Epstein and Kustin noted several deficiencies, and it was soon superseded by another that has since become standard.

The successor mechanism, developed by Citri and Epstein,[8] consists of just eight reactions, one rapid equilibrium, and eight reactive species. The Citri−Epstein (CE) mechanism reproduces clock behavior, bistability, and oscillations, including periods and waveforms. Excitability and hysteresis between the high-iodide steady state and oscillations are also predicted by the model.[9] However, discrepancies remained and agreement came at a price. For instance, the rate constant for a reaction involving HIO_2 was altered significantly from its experimental value; expected reactions, such as $HClO_2 + HIO_2$, and species, such as I_3^-, were omitted; and $HClO_2$ and ClO_2^- were assigned identical reactivities toward I^-.

The limitations of both these mechanisms are a consequence of the methodology used to develop them, that is, fine-tuning rate constants for a chosen set of reactions in order to match the dynamics at selected compositions and flow rates. These mechanisms "used neither rate constant determinations by parameter fitting to experiments nor direct kinetics measurements of elementary reactions; essentially these studies were qualitative descriptions of oscillations in the chlorite−iodide reaction."[10]

A more systematic approach was adopted in a third attempt, albeit for a closely related reaction system. In this mechanism, developed by Lengyel, Li, Kustin, and Epstein,[10] the chlorine-containing feedstream species is chlorine dioxide, not chlorite. The open-system ClO_2−I^- reaction had recently been found to be oscillatory and was preferred over the ClO_2^-−I^- system for two reasons: First, chlorine dioxide is more easily purified than sodium chlorite. Second, the ClO_2^-−I^- batch reaction can suffer from irreproducible kinetics, attributed to imperfect mixing compounded by iodide inhibition;[10,11] this complication can be more easily managed for the ClO_2−I^- reaction. To build their mechanism, Lengyel et al. used spectrophotometry to study the

* To whom correspondence should be addressed. E-mail: sattar@bard.edu (S.S.); Robert.Olsen@stockton.edu (R.J.O.).

10.1021/jp0457895 CCC: $30.25
Published on Web 02/12/2005

TABLE 1: Reactions and Associated Kinetic Parameters for the Chlorine Dioxide−Iodide Reaction (LLKE mechanism)[10] [a]

	reaction	rate law
M1	$ClO_2 + I^- \rightarrow ClO_2^- + 1/2\ I_2$	$6 \times 10^3[ClO_2][I^-]$
M2a	$I_2 + H_2O \rightleftarrows HOI + I^- + H^+$	$1.98 \times 10^{-3}[I_2]/[H^+] - 3.67 \times 10^9[HOI][I^-]$
M2b	$I_2 + H_2O \rightleftarrows HOI + I^- + H^+$	$5.52 \times 10^{-2}[I_2] - 3.48 \times 10^9[H_2OI^+][I^-]$
M3	$HClO_2 + I^- + H^+ \rightarrow HOI + HOCl$	$7.8[HClO_2][I^-]$
M4	$HClO_2 + HOI \rightarrow HIO_2 + HOCl$	$6.9 \times 10^7[HClO_2][HOI]$
M5	$HOCl_2 + HIO_2 \rightarrow IO_3^- + HOCl + H^+$	$1.0 \times 10^6[HClO_2][HIO_2]$
M6	$HOCl + I^- \rightarrow HOI + Cl^-$	$4.3 \times 10^8[HOCl][I^-]$
M7	$HOCl + HIO_2 \rightarrow IO_3^- + Cl^- + 2H^+$	$1.5 \times 10^3[HOCl][HIO_2]$
M8	$HIO_2 + I^- + H^+ \rightleftarrows 2HOI$	$1.0 \times 10^9[HIO_2][I^-][H^+] - 22[HOI]^2$
M9	$2HIO_2 \rightarrow IO_3^- + HOI + H^+$	$25[HIO_2]^2$
M10	$HIO_2 + H_2OI^+ \rightarrow IO_3^- + I^- + 3H^+$	$1.1 \times 10^2[HIO_2][H_2OI^+]$
M11	$HOCl + Cl^- + H^+ \rightleftarrows Cl_2 + H_2O$	$2.2 \times 10^4[HOCl][Cl^-][H^+] - 22[Cl_2]$
M12	$Cl_2 + I_2 + 2H_2O \rightarrow 2HOI + 2Cl^- + 2H^+$	$1.5 \times 10^5[Cl_2][I_2]$
M13	$Cl_2 + HOI + H_2O \rightarrow HIO_2 + 2Cl^- + 2H^+$	$1.0 \times 10^6[Cl_2][HOI]$
M14	$HClO_2 \rightleftarrows ClO_2^- + H^+$	$2 \times 10^9[HClO_2] - 1 \times 10^{11}[H^+][ClO_2^-]$
M15	$H_2OI^+ \rightleftarrows HOI + H^+$	$3.4 \times 10^9[H_2OI^+] - 1 \times 10^{11}[H^+][HOI]$
M16	$I_2 + I^- \rightleftarrows I_3^-$	$6.2 \times 10^9[I_2][I^-] - 8.5 \times 10^6[I_3^-]$

[a] Reaction M1 is the only reaction involving ClO_2. Reactions M14−M16 are rapid equilibria. Concentrations are expressed in moles per liter and rates in moles per liter per second.

kinetics of the overall reaction and four subsystems: $HClO_2 + I_2$, $HOCl + I_2$, HIO_2 disproportionation, and HOI disproportionation. Using least-squares fitting of the kinetics curves and sensitivity analysis and proceeding from simpler to more complex fragments of the overall reaction, they identified a set of reactions and rate equations that best described each subsystem and the overall reaction. Their mechanism, given in Table 1, consists of thirteen reactions, three rapid equilibria, and thirteen reactive species. When this mechanism was used to model the open-system reaction between ClO_2 and I^-, the calculated phase diagram in an $[I^-]_0-k_0$ plane and the calculated variation of the oscillation period with flow rate essentially duplicated experimental results.[10,12] It is important to appreciate that agreement with the open-system reaction required no adjustment of previously determined rate and equilibrium constants; the model was constructed using rate laws from kinetic studies of the closed system only.

All the flaws in the CE mechanism noted above were corrected and I_3^-, H_2OI^+, Cl^-, and Cl_2 were added to the list of reactive species. As was true of the earlier mechanisms, the majority of the reactions in the Lengyel-Li-Kustin-Epstein (LLKE) mechanism are not elementary, the most obvious being iodine hydrolysis (M2a and M2b). The rate expressions for iodine hydrolysis describe parallel paths: the first is acid-inhibited and invokes I_2OH^- as an intermediate, whereas the second invokes H_2OI^+. The mechanism is restricted to the range of conditions over which the kinetics of the ClO_2-I^- reaction and its subsystems were studied; these are $3 < [I^-]_0/[ClO_2]_0 < 5$, $1 < pH < 3.5$, and $T = 298$ K.

Because chlorine dioxide is involved only in the first step of the mechanism, it is natural to ask whether, in the absence of this step, the remaining steps (M2−M16) constitute an improved mechanism of the $ClO_2^--I^-$ reaction, the original system of interest. Lengyel et al. allude to the notion that experimental oscillations in this system arise from inhomogeneities by reporting that their model "did not produce homogeneous oscillations where stirring and mixing effects occur in the chlorite−iodide reaction."[10] Before the authenticity of oscillations in the $ClO_2^--I^-$ reaction is cast more deeply into doubt, we feel that the validity of the LLKE mechanism as it applies to this reaction must be tested under a broad variety of conditions, not just those expected to produce oscillations.

We depart from the LLKE mechanism in small respects. In their implementation, Lengyel et al. use the equilibrium constraints M14−M16 to reduce the number of concentration variables by three.[10] Instead, we assign rate constants to the forward and reverse steps of these equilibria. For protonation reactions, we use diffusion-limited rate constants. For M16, we use literature values of the forward and reverse rate constants.[13] These give $K_{M16} = 730$ rather than 740, an insignificant difference. We confirmed that quasi-equilibrium among the relevant species was maintained in all three cases. For completeness, we include M11−M13 in all our calculations, even though they are expected to be negligible for $pH > 2.0$ and $[HClO_2] < 10^{-3}$ M.

Methods

The rate equations were integrated numerically using a version of the Gear method[14] with a finite-difference Jacobian. Steady states of the rate equations for open systems were tracked as functions of the parameters using pseudo-arclength continuation[15] (initial steady states for these calculations were computed by numerical integration). Successful continuation of steady states requires putting species' concentrations on a logarithmic scale and using an analytic Jacobian. All calculations were done in double precision arithmetic.

Results

Closed-System Reaction. Conditions under which the chlorite−iodide reaction displays clock behavior are a logical starting point to evaluate the mechanism. Ten concentration versus time curves have been published,[1,16−18] but only five are within or near the pH range over which the LLKE mechanism is reliable. A selection of these is shown in Figure 1, along with predictions of the mechanism. The shapes of the curves are unmistakably similar, peak iodine concentrations are in generally good agreement, and the mechanism reproduces the observed recovery of I_2 after the clock time, yet there are disparities in clock times and iodine concentrations near the beginning and at the end of the reaction.

For curves (a) and (b) in Figure 1, the calculated clock times are shorter than those found experimentally.[18] Furthermore, as the initial chlorite concentration is decreased, the difference between experimental and calculated clock times increases. (This trend includes two traces at intermediate chlorite concentrations omitted from Figure 1.)

For curve (c), the predicted clock time is longer than the experimental value.[1] In this case, sodium chlorite was used as supplied, calling its concentration into question. If one corrects

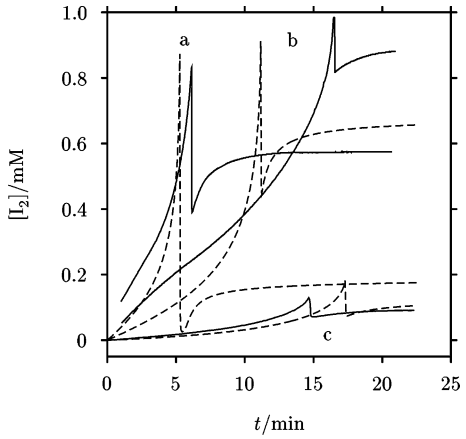

Figure 1. Experimental and calculated kinetics curves for the closed-system ClO_2^-−I^- reaction. (a) $[I^-]_0 = 2.0$ mM, $[ClO_2^-]_0 = 2.5$ mM, and pH = 3.40; (b) $[I^-]_0 = 2.0$ mM, $[ClO_2^-]_0 = 1.25$ mM, and pH = 3.40; and (c) $[I^-]_0 = 0.4$ mM, $[ClO_2^-]_0 = 0.25$ mM, and pH = 3.3. In each pair, experimental data are drawn with solid lines and calculated curves with dashed lines. Data for (a) and (b) are from ref 18 and for (c) from ref 1.

TABLE 2: Comparison of Clock Times for the Chlorite−Iodide Reaction[a]

	clock time/s	
$[I^-]_0$/mM	experimental	calculated
0.3333	85	84
0.6666	110−180	141
1.333	300	240
3.333	580	476
8.333	1200	936
25	3400	

[a] For all trials, $[ClO_2^-]_0 = 5.0$ mM and $[H^+] = 0.0875$ mM. Experimental values are estimated from Figure 1 in ref 11. Variability of the clock times at $[I^-]_0 = 0.6666$ mM is ascribed to a particular interaction of mixing efficiency and reaction kinetics. At $[I^-]_0 = 25$ mM, the simulated reaction does not show clock behavior.

for this assuming 80% $NaClO_2$ and 20% NaCl by mass (a typical composition of commercially available $NaClO_2$), the calculated clock time becomes even longer and the maximum iodine concentration higher than observed, so an erroneous ClO_2^- concentration cannot account for the difference.

We also made a comparison with the results of an exhaustive study of the reproducibility of the ClO_2^-−I^- reaction[11] in which clock times were measured 50 or more times each for a series of compositions at a pH of about 4. Average clock times estimated from Figure 1 in ref 11 together with calculated values are listed in Table 2. If one bears in mind that the pH lies 0.5 units above the reliable range of the LLKE mechanism, the calculated clock time is in good agreement with the experimental value at the largest $[ClO_2^-]_0/[I^-]_0$ ratio, but differs substantially in all other cases. Comparison is unfortunately restricted to just this aspect of the reaction, as representative kinetic curves are not shown.

Thus, although the LLKE mechanism is a quantitatively accurate model of the ClO_2−I^- clock reaction, it is only a qualitatively accurate model of the ClO_2^-−I^- clock reaction.

Open-System Reaction. Despite the long history of the ClO_2^-−I^- reaction, just four experimental phase diagrams at 298 K have been reported: one $[I^-]_0$− pH plane, two $[I^-]_0$−$[ClO_2^-]_0$ planes, and one $[ClO_2^-]_0/[I^-]_0$−k_0 plane. We have simulated each of these using the LLKE mechanism.

We start with a comparison of behavior in the $[I^-]_0$−pH plane at fixed input chlorite concentration and flow rate. Experimentally, the phase diagram shows a wide region of bistability

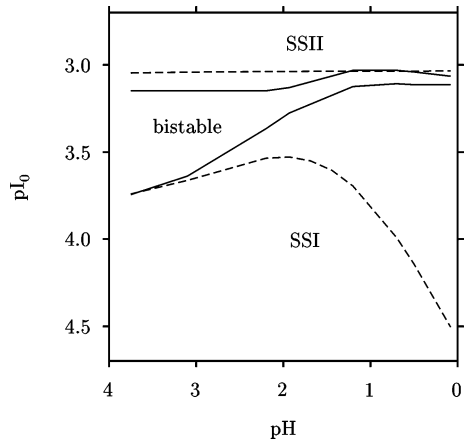

Figure 2. Phase diagram in the $[I^-]_0$−pH plane with $[ClO_2^-]_0 = 0.25$ mM and $k_0 = 5.4 \times 10^{-3}$ s^{-1}. SSI denotes the low-iodide, high-conversion steady state. SSII denotes the high-iodide, low-conversion steady state. Experimental data[1] are drawn with solid lines and calculated curves with dashed lines. Note that pH = 1 is the lower limit of the valid range of the LLKE mechanism.

TABLE 3: Reactions for the Decomposition of Chlorous Acid in the pH Range 0.7−1.9[19]

D1	$2HClO_2 \rightleftarrows Cl_2O_3 + H_2O$
D2	$Cl_2O_3 + H_2O \rightarrow HOCl + ClO_3^- + H^+$
D3	$Cl_2O_3 + Cl^- + H^+ \rightarrow Cl_2O_2 + HOCl$
D4	$Cl_2O_3 + HClO_2 + H_2O \rightarrow Cl^- + 2ClO_3^- + 3H^+$
D5	$HClO_2 + HOCl \rightarrow Cl_2O_2 + H_2O$
D6	$Cl_2O_2 + ClO_2^- \rightarrow Cl^- + 2ClO_2$
D7	$Cl_2O_2 + H_2O \rightarrow Cl^- + ClO_3^- + 2H^+$
D8	$ClO_2^- + Cl_2O_2 + H_2O \rightarrow 2HOCl + ClO_3^-$
D9	$HClO_2 + Cl^- + H^+ \rightarrow 2HOCl$

between the low-iodide and high-iodide steady states (designated SSI and SSII, respectively) that narrows as pH is decreased.[1] Figure 2 illustrates that, like the experimentally determined boundary, the calculated boundary of the bistable region with SSII is insensitive to pH, and the boundaries match very well. However, the experimental and calculated boundaries of the bistable region with SSI are very different. Agreement is good at the upper end of the pH range, but the boundaries diverge rapidly for pH < 2, thus widening the predicted region of bistability. It is not surprising that the upper boundary is nearly insensitive to pH, as the extent of reaction in SSII is small. At the lower boundary, where the extent of reaction is greater, the sensitivity of the reaction rates to $[H^+]$ manifests itself. Of the thirteen pertinent rate laws (M2−M13) in Table 1, only three contain $[H^+]$ explicitly, but the rates of six other reactions are affected by pH through shifts in the $[ClO_2^-]/[HClO_2]$ and $[HOI]/[H_2OI^+]$ ratios.

We appended a detailed mechanism for the decomposition of chlorous acid[19] to the LLKE mechanism to investigate whether this might account for the inaccurate predictions at low pH. (Decomposition of chlorous acid is known to occur under acidic conditions and ultimately yields ClO_3^-, ClO_2, and Cl^-.) Homolytic cleavage of $HClO_2$ to HO· and ClO· and reactions involving these radicals are neglected, as these reactions are unimportant for time periods shorter than 1 day. Reactions D1 and D5 (Table 3) initiate the decomposition pathway by generating Cl_2O_3 and Cl_2O_2. No reactions of iodine-containing species with these new intermediates were considered; as ClO_2 is a product of D6, M1 is now included.

Grafting the reactions of Table 3 onto the LLKE mechanism alters the boundaries of the bistable region of Figure 2 only slightly. The impact of the additional reactions is negligible at $[H^+] = 1.8 \times 10^{-4}$ M and shrinks the bistable region by about

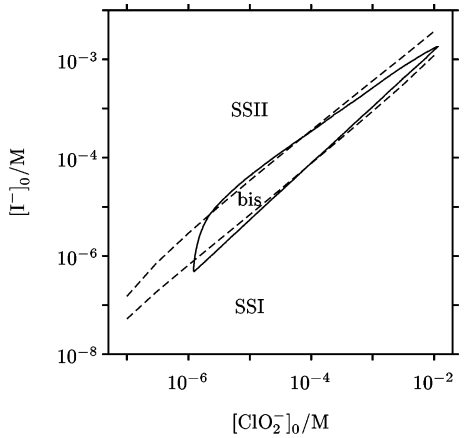

Figure 3. Phase diagram in the $[I^-]_0-[ClO_2^-]_0$ plane at pH = 3.35 and $k_0 = 5.4 \times 10^{-3}$ s^{-1}. Experimental data[1] are drawn with solid lines and calculated curves with dashed lines.

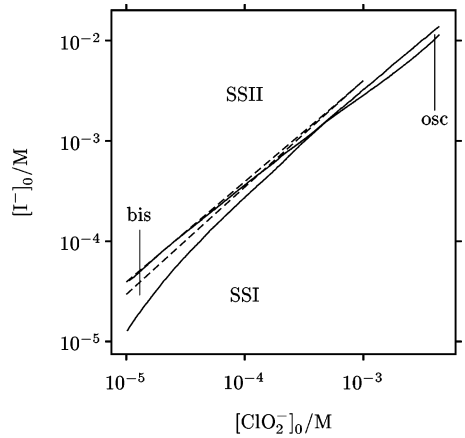

Figure 4. Phase diagram in the $[I^-]_0-[ClO_2^-]_0$ plane with pH = 2.04 and $k_0 = 1.1 \times 10^{-3}$ s^{-1}. Experimental data[1] are drawn with solid lines and calculated curves with dashed lines.

1% at $[H^+] = 0.83$ M. Consideration of reaction rates at $[H^+] = 0.83$ M reveals why the $HClO_2$ decomposition pathway is not significant.

Under conditions of low iodide consumption, $D1_{fwd}$ is faster than any other reaction involving $HClO_2$ (M3−M5, D4, D5, D9) and the rate of $D1_{rev}$ is at least 4 orders of magnitude greater than the rates of D2−D4, so D1 is essentially at equilibrium. Because the equilibrium constant of D1 is 0.01 and $[HClO_2]$ is at most 2.5×10^{-4} M, $[Cl_2O_3]$ does not exceed 10^{-9} M. Formation of Cl_2O_3 ($D1_{fwd}$), D5, and D9 hardly decrease $[HClO_2]$, and the rates of M3−M5 are hardly altered. Reaction D5 is at least 3 orders of magnitude slower than M6, so the dominant pathway for HOCl consumption remains the reaction between HOCl and iodine-containing species. The rates of M2−M16 are nearly the same whether or not decomposition of $HClO_2$ is taken into account, and the transition from the low-conversion to the high-conversion steady state occurs at nearly the same value of $[I^-]_0$.

Under conditions of high iodide consumption, D1 is again essentially at equilibrium. The dominant pathway for the reaction between $HClO_2$ and iodine-containing species is now M4 and M5 rather than M3 and M4. For $[I^-]_0 > 0.2$ mM, D5 is at least 2 orders of magnitude slower than M5 and at least 3 orders of magnitude slower than M4, and $D1_{fwd}$, D4, and D9 are several orders of magnitude slower still. The net reaction of $HClO_2$ consequently takes place as in the absence of the decomposition pathway. The dominant pathway for HOCl consumption continues to be the reaction between HOCl and iodine-containing species, because D5 is at least 2 orders of magnitude slower than M6 or M7 (or both). As before, the rates of M2−M16 are nearly the same whether or not decomposition of $HClO_2$ is taken into account, and the transition from the high-conversion to the low-conversion steady state occurs at nearly the same value of $[I^-]_0$. Only under conditions of high iodide consumption and $[I^-]_0 < 0.2$ mM does chlorous acid decomposition become important, and these conditions are remote from the corresponding boundary of the bistable region.

In the $[I^-]_0-[ClO_2^-]_0$ plane at pH = 3.35 (Figure 3), the predictions of the model are in close agreement with the experimental boundary between the bistable region and SSI, though the calculated bistable region is again more extensive than observed.[1] At pH = 2.04 (Figure 4), the model agrees less well with reported behavior.[1] Only an exceedingly narrow range of bistability is predicted, and oscillations are absent. As the flow rate is increased in the simulations, the V-shaped region of bistability opens up and the hysteresis limit shifts to higher $[I^-]_0$ and $[ClO_2^-]_0$, but we found no oscillatory region beyond this point.

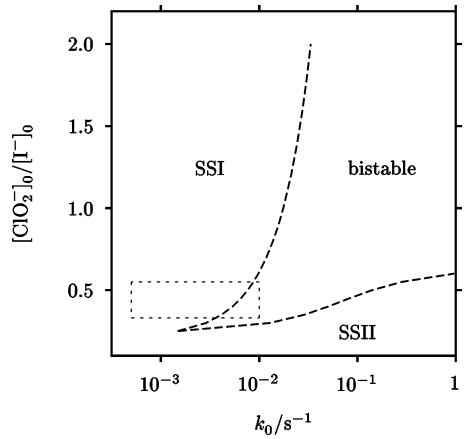

Figure 5. Calculated phase diagram in the $[ClO_2^-]_0/[I^-]_0-k_0$ plane at pH = 2.05. Oscillatory behavior was observed experimentally in the region outlined by the rectangle.[3]

A fourth comparison is made at fixed pH in the $[ClO_2^-]_0/[I^-]_0-k_0$ plane. The model predicts a large bistable region, but oscillations are again absent from the region where they were found experimentally,[3] as shown in Figure 5. The bistable region was not delineated in these experiments, because this study focused on oscillatory dynamics. Consequently, the predictions of the model regarding bistability cannot be tested.

As noted in the Introduction, the chlorite−iodide reaction is sensitive to premixing. For instance, when three reagent feedstreams ($[ClO_2^-]_0 = 1.0$ mM, $[I^-]_0 = 3.6$ mM, pH = 2.0) were premixed, instead of showing oscillations (as in the absence of premixing), the system resided in either the low- or middle-iodide steady state, depending on flow rate.[2] Our simulations also show that the system resides in one of two steady states, this time low- or high-iodide, with hysteresis. This result suggests that the model, which assumes that the solution is homogeneous, might more accurately reflect experiments in which the reagents are combined before they enter the CSTR. However, oscillations found in such an experiment ($[ClO_2^-]_0 = 0.5$ mM, $[I^-]_0 = 1.8$ mM, pH = 1.56)[2] were replaced by a bistable state in our simulations.

Discussion

We consider our most significant result to be the absence of oscillations from the simulations of the ClO_2^-−I^- reaction using

TABLE 4: Rate Laws for the LLKE[10] and CE[8] Mechanisms at $[H^+] = 1.0 \times 10^{-2}$ M[a]

	LLKE mechanism	CE mechanism
M2	$2.53 \times 10^{-1}[I_2] - 4.69 \times 10^{9}[HOI][I^-]$	$1.3 \times 10^{-1}[I_2] - 4 \times 10^{9}[HOI][I^-]$
M3	$7.8[HClO_2][I^-]$	$10[HClO_2][I^-]$
M4	$6.9 \times 10^{7}[HClO_2][HOI]$	$6 \times 10^{7}[HClO_2][HOI]$
M6	$4.3 \times 10^{8}[HOCl][I^-]$	$1.4 \times 10^{8}[HOCl][I^-]$
M7	$1.5 \times 10^{3}[HOCl][HIO_2]$	$1 \times 10^{3}[HOCl][HIO_2]$
M8	$1.0 \times 10^{7}[HIO_2][I^-] - 22[HOI]^2$	$1 \times 10^{4}[HIO_2][I^-] - 25[HOI]^2$
M9	$25[HIO_2]^2$	$3 \times 10^{3}[HIO_2]^2$
M10	$32[HIO_2][HOI]$	$2.3 \times 10^{2}[HIO_2][HOI]$

[a] Concentrations are expressed in moles per liter and rates in moles per liter per second.

the LLKE mechanism of the ClO_2-I^- reaction. Accordingly, discussion is devoted to the evaluation of two plausible conclusions that come readily to mind: experimentally observed oscillations in the $ClO_2^--I^-$ reaction are due to imperfect mixing and should not be reproduced by the simulations (perfect mixing is implicit in the CSTR model), or revision of the mechanism is necessary.

We investigated whether incorporating the basic model of imperfect mixing of Kumpinsky and Epstein[20] might induce oscillations. The CSTR is notionally divided into two zones, designated active and dead, which are open to each other, but only the active zone is open to the surroundings. The extent of mixing is characterized by two new parameters: the volume fraction of the CSTR occupied by the dead zone, x, and the ratio of the residence times in the active to the dead zone, z. Homogeneity is approached as $x \rightarrow 0$ or as $z \rightarrow \infty$.

Recalculating Figure 4 for typical values[20] of x and z (0.3 and 0.6) leads to only minor changes. The hysteresis limit moves to slightly higher $[I^-]_0$ and $[ClO_2^-]_0$. With $[I^-]_0$ fixed, the bistable interval widens; transitions from low- to high-conversion states occur at essentially the same $[ClO_2^-]_0$, and transitions from high- to low-conversion states occur at somewhat greater $[ClO_2^-]_0$. Again, no oscillatory region was found.

To explore further the impact of imperfect mixing on the CSTR dynamics of the chlorite−iodide reaction, we fixed k_0 and pH at the values of Figure 4, chose $[I^-]_0 = 1.0 \times 10^{-2}$ M and $[ClO_2^-]_0 = 3.5 \times 10^{-3}$ M, a point squarely in the oscillatory region of Figure 8 of ref 1, and tracked the steady state as a function of x for several values of z. If the active and dead zones are strongly coupled ($z = 1$ and $z = 10$) and the dead zone is not too large ($x < 0.75$), the active zone is in the high-conversion state, just as in the perfectly mixed CSTR.

For $z = 0.6$, a mushroom[21] exists in the interval $0.968 \leq x \leq 0.994$, and oscillations are observed on a smaller interval ($0.969 \leq x \leq 0.991$) in the interior of the mushroom. The mushroom persists as z is decreased, and an isola[21] of steady states appears in which the active zone is in the high-iodide state. At $z = 0.4$, the smallest value investigated, the isola begins at $x = 0.781$. It is unlikely that this isola and the one observed experimentally upon variation of flow rate[6] are related, because isola formation depends critically on designation of a distinguished parameter. No attempt was made to complete the $x-z$ phase diagram by performing a full analysis of the dynamics in this plane, as values of x and z for which new dynamics is observed correspond to risibly poor mixing.

While this attempt to explain the absence of oscillations does not provide evidence for the view that they arise from imperfect mixing, the use of more sophisticated mixing models[22,23] might. Should this happen, such mixing models ought to be incorporated into the closed-system model in an effort to reconcile the quantitative discrepancies between experiment and simulation. We do not believe these to be a reflection of the known irreproducibility of clock times in the chlorite−iodide reaction, as this occurs in a small minority of cases involving particular combinations of solution composition and mixing efficiency,[11] and one must assume that the experimenters were satisfied with the reproducibility of the kinetic curves in Figure 1. Moreover, the steady increase in the difference between our calculated clock times and those reported in ref 18 as $[ClO_2^-]_0$ is decreased would be improbable if experimental clock times were highly variable.

We now turn from mixing to the mechanism. Species or reactions that are unimportant in the $ClO_2^--I^-$ reaction might be important in the $ClO_2^--I^-$ reaction, so revision could entail not only adjustment of rate constants but also inclusion of new reactions or inclusion of new species and their reactions. For example, in deriving the rate law for M2a, Lengyel et al.[10] eliminated I_2OH^- by applying the quasi-steady-state approximation to this intermediate and confirmed that there was no effect on the ClO_2-I^- reaction in the closed system. We were concerned that this approximation might not be valid in the $ClO_2^--I^-$ reaction, particularly in a CSTR. However, upon replacing M2a by three reversible reactions that include I_2OH^- explicitly,[10,24] we found a negligible effect on the clock behavior shown in Figure 1 and on the phase diagram shown in Figure 4.

Because the CE mechanism generates oscillations, comparison with the LLKE mechanism is helpful. All eight reactions in the CE mechanism are included in the LLKE mechanism, with two qualifications. First, in the CE mechanism, $[ClO_2^-] + [HClO_2]$ replaces $[HClO_2]$ in the rate law for M3. Second, the CE mechanism does not consider protonation of HOI (M15) and therefore uses HOI in place of H_2OI^+ in M10. Not all reactions added by Lengyel et al.[10] are equally important: according to the guidelines accompanying Table 1 of ref 10, reactions M11−M13 will have a minor impact under the conditions at which the CE mechanism exhibits oscillatory dynamics.[8] We note that Citri and Epstein reported that inclusion of M16 did not affect their results.

Because the $[H^+]$ dependence of several rate laws complicates direct comparison of the two mechanisms, we simplify matters by making the comparison at $[H^+] = 1.0 \times 10^{-2}$ M, an optimal concentration for producing oscillations (see Table 4). To facilitate direct comparison, rate laws for the two iodine hydrolysis pathways (M2a, M2b) have been combined, and the rate law for M10 has been expressed in terms of [HOI]. At this H^+ concentration, seven rate constants ($M2_{fwd}$, $M2_{rev}$, M3, M4, M6, M7, $M8_{rev}$) in the two models are within a factor of 3 of each other, but three ($M8_{fwd}$, M9, M10) differ by factors ranging from nearly 10 to 1000. That all three reactions involve HIO_2, as does M5, a reaction absent from the CE mechanism, is noteworthy. Citri and Epstein found both batch and oscillatory behavior of the $ClO_2^--I^-$ reaction acutely sensitive to HIO_2 levels. It is for this reason that they excluded M5, altered the rate constant for M9 from its reported value, and set the rate constant for $M8_{fwd}$ at the lower limit of its reported range.

Lengyel et al.[10] include M5 and restore the rate constant for M9 to an experimentally determined value; this is intuitively desirable, as is their method of building more complex reaction networks from simpler ones. However, combustion chemistry provides examples in which a large reaction network assembled from smaller ones does not accurately predict the full range of observed dynamics.[25] In this light, reproduction of the CSTR dynamics of the ClO_2-I^- reaction without adjustment of the rate constants found entirely from closed system experiments is remarkable. Nevertheless, it would be interesting to reevaluate the rate constants of the LLKE mechanism by including these CSTR results[12] in the optimization procedure. Owing to the discrepancies illustrated by Figure 1, including chlorite−iodide clock reactions among the target experiments is appropriate. New methods of model development[26,27] applied to such an enlarged training set should yield a mechanism that not only retains the strengths of the LLKE mechanism but also accurately captures those aspects of chlorite−iodide reaction dynamics untainted by mixing effects.

Acknowledgment. We thank P. De Kepper, I. R. Epstein, G. A. Frerichs, and M. Orbán for helpful discussions.

References and Notes

(1) Dateo, C. E.; Orbán, M.; De Kepper, P.; Epstein, I. R. *J. Am. Chem. Soc.* **1982**, *104*, 504.
(2) Luo, Y.; Epstein, I. R. *J. Chem. Phys.* **1986**, *85*, 5733.
(3) Stemwedel, J. D.; Ross, J. *J. Phys. Chem.* **1993**, *97*, 2863.
(4) Menzinger, M.; Boissonade, J.; Boukalouch, M.; De Kepper, P.; Roux, J. C.; Saadaoui, H. *J. Phys. Chem.* **1986**, *90*, 313.
(5) Boukalouch, M.; Boissonade, J.; De Kepper, P. *J. Chim. Phys. Phys.-Chim. Biol.* **1987**, *87*, 210.
(6) Ali, F.; Menzinger, M. *J. Phys. Chem.* **1991**, *95*, 6408.
(7) Epstein, I. R.; Kustin, K. *J. Phys. Chem.* **1985**, *89*, 2275.
(8) Citri, O.; Epstein, I. R. *J. Phys. Chem.* **1987**, *91*, 6034.
(9) Strasser, P.; Stemwedel, J. D.; Ross, J. *J. Phys. Chem.* **1993**, *97*, 2851.
(10) Lengyel, I.; Li, J.; Kustin, K.; Epstein, I. R. *J. Am. Chem. Soc.* **1996**, *118*, 3708.
(11) Nagypál, I.; Epstein, I. R. *J. Chem. Phys.* **1988**, *89*, 6925.
(12) Lengyel, I.; Li, J.; Epstein, I. R. *J. Phys. Chem.* **1992**, *96*, 7302.
(13) Turner, D. H.; Flynn, G. W.; Sutin, N.; Beitz, J. V. *J. Am. Chem. Soc.* **1972**, *94*, 1554.
(14) Hindmarsh, A. C. *GEAR. Ordinary Differential Equation System Solver*; Technical Report UCID-30001 Rev. 3; Lawrence Livermore Laboratory: Livermore, CA, 1974.
(15) Doedel, E. J.; Champneys, A. R.; Kuznetsov, T. F. F. Y. A.; Sandstede, B.; Wang, X. *AUTO97: Continuation and Bifurcation Software for Ordinary Differential Equations (with HomCont)*; 1998; http://indy.cs.concordia.ca/auto/.
(16) Kern, D. M.; Kim, C.-H. *J. Am. Chem. Soc.* **1965**, *87*, 5309.
(17) de Meeus, J.; Sigalla, J. *J. Chim. Phys. Phys.-Chim. Biol.* **1966**, *63*, 453.
(18) Beck, M. T.; Rábai, G. *J. Phys. Chem.* **1986**, *90*, 2204.
(19) Horváth, A. K.; Nagypál, I.; Peintler, G.; Epstein, I. R.; Kustin, K. *J. Phys. Chem. A* **2003**, *107*, 6966.
(20) Kumpinsky, E.; Epstein, I. R. *J. Chem. Phys.* **1985**, *82*, 53.
(21) Gray, P.; Scott, S. K. *Chemical Oscillations and Instabilities: Nonlinear Chemical Kinetics*; The International Series of Monographs on Chemistry; Oxford University Press: Oxford, 1990; Vol. 21.
(22) Fox, R. O.; Villermaux, J. *Chem. Eng. Sci.* **1990**, *45*, 2857.
(23) Fox, R. O.; Erjaee, G.; Zou, Q. *Chem. Eng. Sci.* **1994**, *49*, 3465.
(24) Lengyel, I.; Epstein, I. R.; Kustin, K. *Inorg. Chem.* **1993**, *32*, 5880.
(25) Frenklach, M.; Wang, H.; Rabinowitz, M. J. *Prog. Energy Combust. Sci.* **1992**, *18*, 47.
(26) Frenklach, M.; Packard, A.; Seiler, P.; Feeley, R. *Int. J. Chem. Kinet.* **2004**, *36*, 57.
(27) Davis, S. G.; Mhadeshwar, A. B.; Vlachos, D. G.; Wang, H. *Int. J. Chem. Kinet.* **2004**, *36*, 94.